PNAS
www.pnas.org

Supplementary Information for

The nutrient sensor OGT regulates Hipk stability and tumorigenic-like activities in *Drosophila*

Kenneth Kin Lam Wong, Ta-Wei Liu, Jessica M. Parker, Donald A.R. Sinclair, Yi-Yun Chen, Kay-Hooi Khoo, David J. Vocadlo, Esther M. Verheyen

Esther M. Verheyen
Email: everheye@sfu.ca

This PDF file includes:

www.pnas.org/cgi/doi/10.1073/pnas.1912894117

SI Materials and Methods

Fly food recipes

Regular cornmeal-molasses fly food containing 0.8 g agar, 2.3 g yeast, 5.7 g cornmeal and 5.2 mL molasses per 100 mL was used. Control diet (also known as low sucrose diet (LSD)) and High sucrose diet (HSD) have been previously described (1). Briefly, control diet referred to semi-defined food containing 1 g agar, 8 g Brewer's yeast, 2 g yeast extract, 2 g peptone, 5.1 g sucrose per 100 mL. HSD contained 1 g agar, 8 g Brewer's yeast, 2 g yeast extract, 2 g peptone, 34.2 g sucrose per 100 mL. Glucosamine supplemented food was prepared by adding glucosamine to control semi-defined food at a final concentration of 0.1 M.

Fly strains

The following fly strains were used: *dpp-Gal4*, *dpp-Gal4 UAS-HA-hipk^{3M}* (abbreviated as *dpp>hipk*) (2), *en-Gal4 UAS-GFP*, *actin5c-Gal4* (BL 3954), U*AS-HA-hipk^{3M}* (3), *UAS-ogt-RNAi* (VDRC 18610), *UAS-ogt-RNAi* #2 (2824-1) (4), *UAS-ogt-flag* (D. Sinclair), *UAS-ogt* (4), *UAS-GFP* (BL 5431), *UAS-RFP* (BL 7118), *UAS-gfat1* (D. Sinclair), *UAS-gfat2* (gift from Linda Partridge), *UAS-gfat1-RNAi* (D. Sinclair), *UAS-gfat1-RNAi* (VDRC 24539), *UAS-gfat2-RNAi* (VDRC 105129), *UAS-gfat2-RNAi* (BL 34740), *UAS-hipk-RNAi* (VDRC 108254). The BL lines were obtained from Bloomington *Drosophila* Research Centre. The VDRC lines were obtained from Vienna *Drosophila* RNAi Centre. The *ogt* null alleles *sxc^{4}*, *sxc^{5}*, *sxc^{6}* and *sxc^{7}* have been described (4, 5).

Immunofluorescence microscopy

After fixation, samples were washed with PBS with 0.1% Triton X-100 (PBST). After blocking with 5% BSA in PBST for 1 hour at room temperature, samples were incubated with primary antibodies overnight at 4°C. The primary antibodies used include rabbit anti-phospho-Histone H3 (Ser10) (Cell Signaling Technology 9701), mouse anti-Mmp1 (1:100 DSHB 3A6B4, 1:100 3B8D12, 1:100 5H7B11), rabbit anti-Cyclin E (d-300) (1:100; Santa Cruz sc-33748), rabbit anti-Hipk (1:200) (2), rat anti-DE-Cadherin (1:50, DSHB DCAD2), rabbit anti-OGT (1:100, Santa Cruz sc-32921), rabbit anti-dMyc (d1-717) (1:500, Santa Cruz sc-28207). After washing with PBST, samples were incubated with Cy3- and/or Alexa Fluor 647-conjugated secondary antibodies (1:500, Jackson ImmunoResearch Laboratories, Inc.), DAPI (4',6-Diamidino-2-Phenylindole, Dihydrochloride) (final concentration: 0.2 µg per mL, Invitrogen D1306) for 2 hours at room temperature. Samples were mounted in 70% Glycerol/PBS after wash. Images were taken on a Nikon Air laser-scanning confocal microscope and processed by Image J.

Western blotting

The primary antibodies used include mouse anti-β-Actin (1:5000, Santa Cruz sc-47778), mouse anti-β-Tubulin (1:1000, Abm G098), mouse anti-Flag (1:1000, Sigma F1804), rabbit anti-Hipk (1:2000) (2), mouse anti-Myc (1:1000, Millipore 05-724) and rabbit anti-OGT (1:1000, Santa Cruz sc-32921). HRP (Jackson ImmunoResearch) or fluorescent dye-conjugated secondary antibodies were used.

WGA pull down

WGA enrichment of *O*-GlcNAc modified proteins has been previously described (6). Protein extracts were incubated in a final volume of 1 ml IP buffer (15 mM Hepes pH 7.9, 200 mM KCl, 1.5 mM $MgCl_2$, 0.2 mM EDTA pH 8, 0.25% NP-40, 20% glycerol, 0.3 mM DTT, 1× "Complete" protease inhibitor cocktail, 1 mM PMSF) with 100 µl of a 50% slurry of washed succinylated WGA-agarose resin (Vector Labs) for 12 h at 4°C. Beads were washed with IP buffer containing 0.5 mM DTT and 0.4% NP-40, followed by a 1 h incubation with 1 M GlcNAc (GALAB) on ice to elute resin-bound proteins.

GalNAz feeding and biotin-conjugation reaction

The metabolic labeling of *O*-GlcNAc modified proteins and subsequent chemoselective ligation has been described previously (6). Ac_4GalNAz media was made by adding Ac_4GalNAz (dissolved in DMSO) to standard cornmeal-molasses fly food at 55°C to a final concentration of 100 µM. Control food was made by adding an equal volume of DMSO. Parents mated on the indicated food and the progeny grew up on it since birth. To biotinylate *O*-GlcNAz-modified

proteins, a Staudinger capture reaction using biotinylated phosphine capture reagent (biotin-*azo*-phosphine) was performed. Biotin-*azo*-phosphine was added to the protein extracts (in 1% SDS-PBS) at a final concentration of 200 µM. The mixture was incubated for overnight at room temperature. Unreacted probe was removed by chloroform-methanol purification. Biotinylated proteins were analyzed by Streptavidin (Strvn) blot using Odyssey (LI-COR Biosciences).

GalT labeling

In vitro Galactosyltransferase labeling using the Click-iT *O*-GlcNAc Enzymatic Labeling System (Invitrogen) has been described (6). Briefly, Gal-T1^{Y289L} was incubated with proteins in labeling buffer (containing 20 mM HEPES, pH 7.9; 50 mM NaCl; 2% NP-40; 5.5 mM MnC_2; 25 µM UDP-GalNAz) according to manufacturer's recommendations. Reaction was performed at 4°C under gentle agitation for 24 h. After labeling, proteins were chloroform-methanol precipitated. The proteins were resuspended with 1%SDS, 20 mM HEPES pH 7.9 and iodoacetamide (IAA) was added to a final concentration of 15 mM to block the free cysteine thiols. The mixture was then under gentle agitation for 30 min at room temperature, followed by addition of DBCO-S-S-PEG_3-Biotin (Jena Bioscience) at a final concentration of 40 µM. The incubation of the mixture was protected from light and under gentle agitation for 30 min at room temperature. Excess non-reactive reagents were then removed by chloroform-methanol protein purification. Proteins were resuspended in 1% SDS, 20 mM HEPES pH 7.9 and incubated with streptavidin beads for 1-2 hour at 4°C on a rocking platform. The binding proteins were released by final concentration of 50 mM DTT at 37°C for 30 min, followed by subsequent western blot analyses using 4-20% gradient SDS-PAGE.

In-Gel Digestion

For in-gel trypsin digestion, the 80~200 kDa protein bands from an SDS-PAGE gel were cut into ~1 mm cubes and subjected to in-gel digestion followed by extraction of the tryptic peptides. The excised gel pieces were destained repeatedly in 25 mM ammonium bicarbonate (ABC)/40% acetonitrile (ACN), reduced with 10 mM dithioerythritol for 1 h at 37 °C, and alkylated with 55 mM iodoacetamide at room temperature in the dark for 1 h. The gel slices were then dried and digested first by Lyc-C protease at 37 °C for 3 h, followed by trypsin at 37 °C overnight. The digested peptides were extracted twice with 50% ACN/ 5% trifluoroacetic acid (TFA) and once with ACN. Extracts from each sample were combined and dried down by use of a SpeedVac. Following the digestion, peptide mixtures were desalted on C_{18} StageTips (7), and resuspended in 0.1% formic acid for LC-MS/MS analysis.

Mass spectrometry to map the O-GlcNAcylation sites of HIPK2

LC-MS/MS analysis was performed on a Thermo UltiMate 3000 RSLCnano system connected to a Thermo Orbitrap Fusion™ Lumos™ Tribrid™ Mass Spectrometer (Thermo Fisher Scientific, Bremen, Germany) via a nanospray interface (New Objective, Woburn, MA). Peptide mixtures were loaded onto a PepMap C_{18} column (75 µm ID, 25 cm length, 2 µm particles, pore size 100 Å, Thermo Fisher Scientific) and separated using a 90 min segmented gradient from 5% to 45% solvent B (80 % acetonitrile with 0.1 % formic acid) at a flow rate of 300 nl/min. Solvent A was 0.1% formic acid in water. The mass spectrometer was operated in the data-dependent mode. Briefly, survey scans of peptide precursors from 350 to 1800 *m/z* were performed at 120K resolution with a 2×10^5 ion count target. The Top Speed method was enabled to ensure full MS spectra were acquired every 3 s. Most abundant precursor ions with 2-8 charges above a threshold ion count of 50,000 were selected for data-dependent higher energy collision dissociation (HCD) at a resolution of 30K and a normalized collision energy of 30%. If peaks at *m/z* 138.0545 (HexNAc oxonium fragment ions), or *m/z* 204.0867 (HexNAc oxonium ions) were detected within the top 50 most abundant peaks, a subsequent electron-transfer/higher energy collision dissociation (EThcD) MS/MS scan of the precursor ion was triggered and acquired in the Orbitrap at a resolution of 30K.

All MS and MS/MS raw spectra from each sample were searched against a uniprot human protein database using Byonic v. 2.16.11 (Protein Metrics, San Carlos, CA). The peptide search parameters were as follow: two missed cleavage for full trypsin digestion with fixed

carbamidomethyl modification of cysteine, variable modifications of methionine oxidation, deamidation on asparagine or glutamine residues, and *N*-acetylhexosamine modification of serine and threonine. The peptide mass tolerance was 10 ppm and fragment mass tolerance values for HCD and EThcD spectra were 20 ppm. The maximum number of common and rare modifications were set at two and one, respectively.

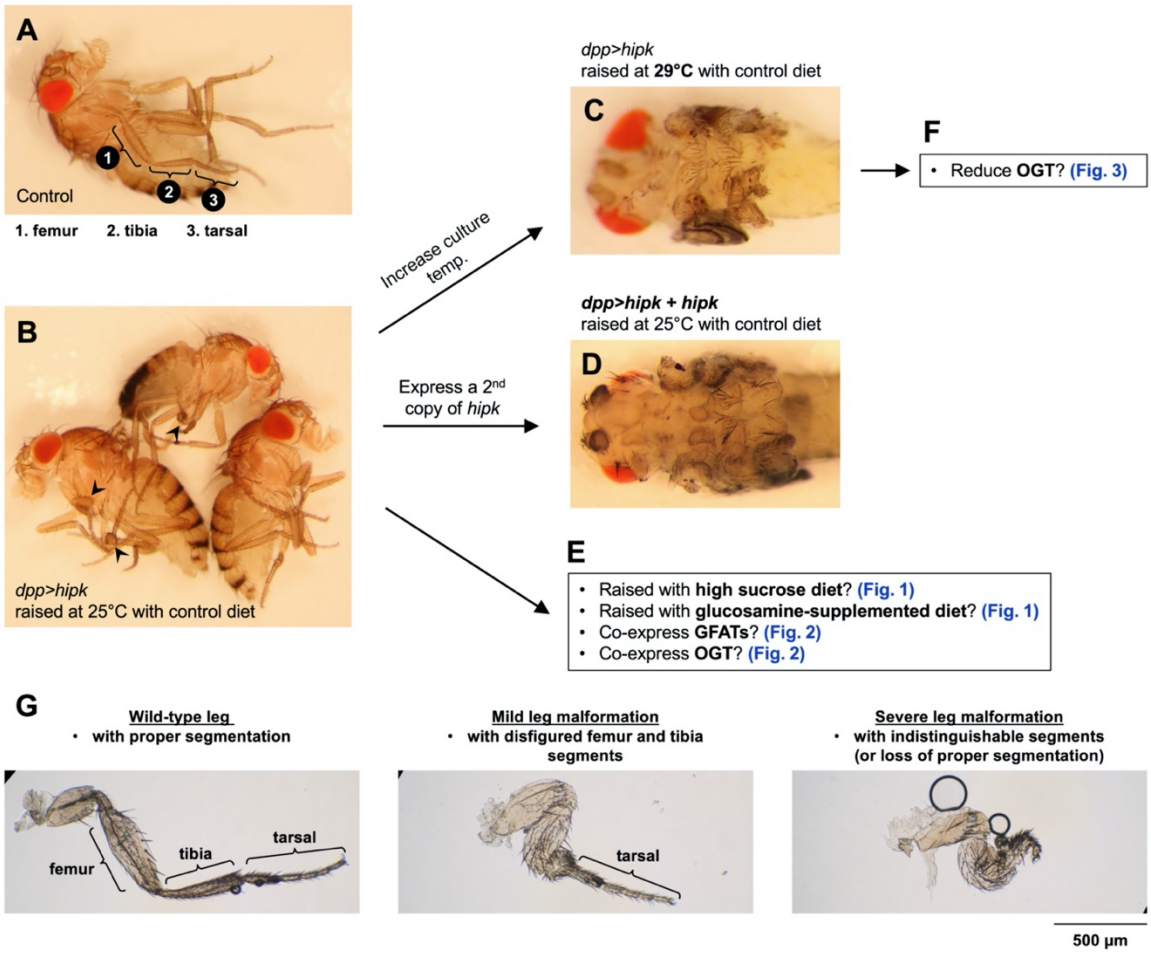

Fig. S1. We used a sensitized Hipk genetic background to investigate potential modifiers of Hipk.

(A) A control fly without *hipk* overexpression (raised at 25°C with control diet) is shown. The adult legs are slender with proper segmentation. Three major segments, femur, tibia and tarsal, are indicated.

(B) Raised at 25°C with control diet, flies overexpressing *hipk* under the control of *dpp-Gal4* driver (which expresses the transgene *hipk* in developing legs) (*dpp>hipk*) usually had a wild-type slender leg phenotype as under these conditions *hipk* is expressed below the threshold to cause any significant growth abnormalities. Occasionally, the flies had one or two legs with deformed segments (arrowheads). We refer this phenotype as a mild leg malformation.

(C-D) Using the sensitized Hipk genetic background described in **(B)**, we further increased Hipk levels by either raising the culture temperature to 29°C (which increases the potency of Gal4 driver thus leading to more transgene expression) **(C)** or expressing a second copy of *hipk* transgene at 25°C **(D)**. High/elevated expression of *hipk* led to formation of legs without proper segmentation. We refer this phenotype as severe leg malformation.

(E) Used the mild leg malformation indicative of moderate *hipk* expression levels **(B)**, we set out to investigate whether Hipk could sense and respond to nutrient signals like high dietary sucrose or glucosamine **(Fig. 1)**. Then, we examined the genetic interactions between Hipk with regulatory enzymes of hexosamine pathway and *O*-GlcNAcylation, GFATs and OGT respectively **(Fig. 2)**.

(F) Using the severe leg malformation indicative of high *hipk* expression levels, we set out to investigate whether OGT is required for Hipk activity **(Fig. 3)**.

(G) Definitions of the leg phenotypes used in this study. A wild-type leg with proper segmentation is shown **(left)**. Mild leg malformation refers to the formation of legs with some distorted segments **(middle)**. Severe leg malformation refers to the formation of legs with significant loss of segmentation **(right)**. Scale bar, 500 μm.

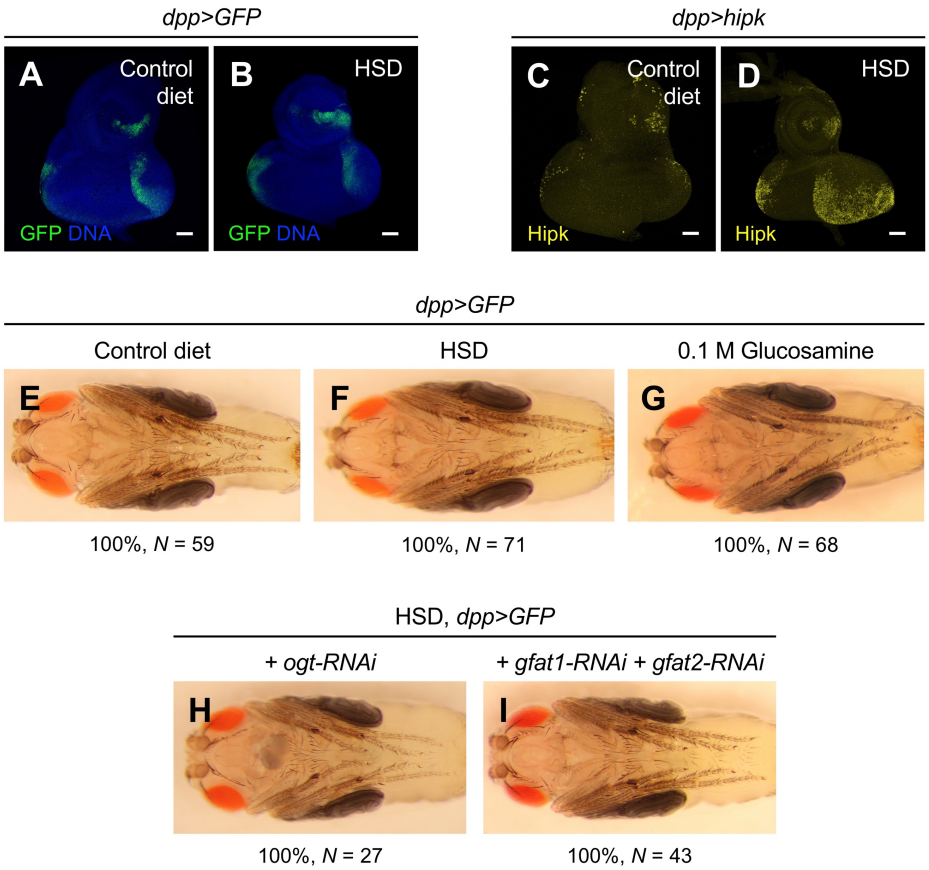

Fig. S2. High dietary sugar promotes cell proliferation and tissue overgrowth in hipk-expressing flies but not in control flies.

Flies were raised at 25°C with the indicated diets.

(A-B) Eye discs expressing GFP (green) in larvae (*dpp>GFP*) fed with either control diet (0.15 M sucrose) **(A)** or high-sucrose diet (HSD, 1 M sucrose) **(B)**. DAPI staining for DNA (blue) shows the overall tissue morphology.

(C-D) Eye discs expressing *hipk* in larvae (*dpp>hipk*) fed with either control diet **(C)** or HSD **(D)**. Eye discs were stained for Hipk (yellow). Scale bar, 50 μm.

(E-G) No abnormal leg phenotypes (as a readout of Hipk activity) were found on control flies (*dpp>GFP*) fed with control diet **(E)**, HSD **(F)** or glucosamine-supplemented diet **(G)** since hatching. Percentages show the phenotype penetrance and *N* is the number of flies counted.

(H-I) No abnormal leg phenotypes were found on flies with genetic inhibition of OGT (*dpp>GFP + ogt-RNAi*) **(H)** or GFATs (*dpp>GFP + gfat1-RNAi + gfat2-RNAi*) **(I)**. Percentages show the phenotype penetrance and *N* is the number of flies counted.

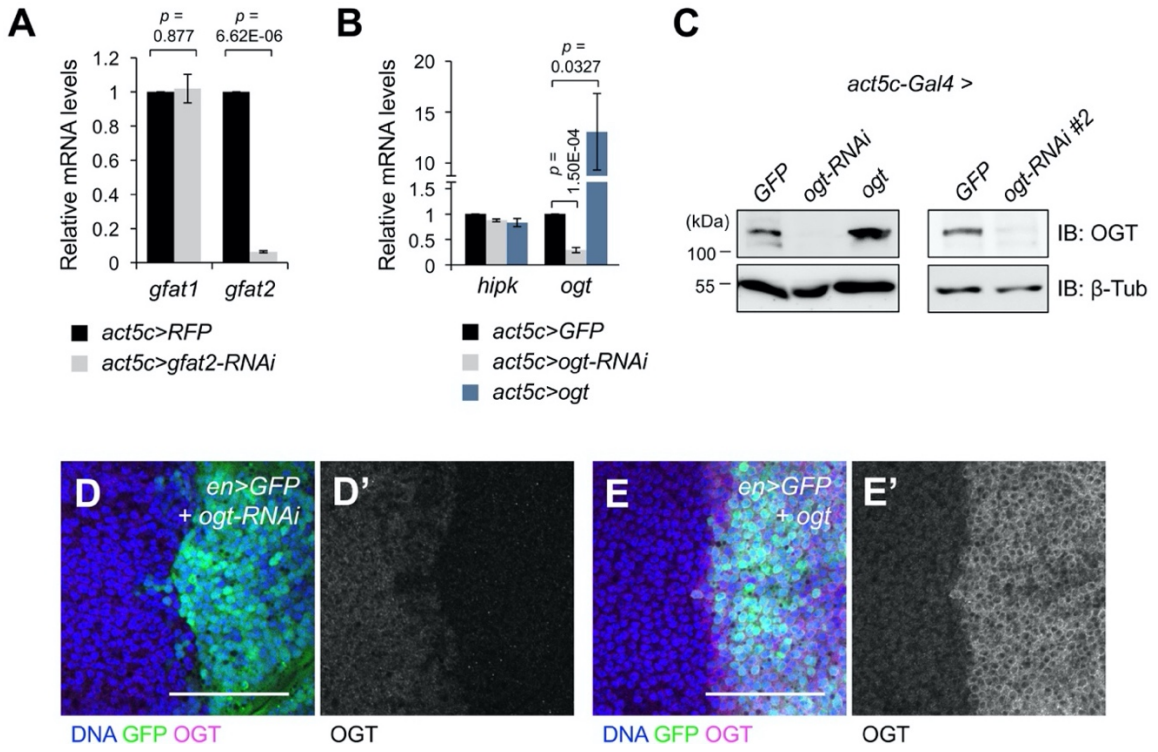

Fig. S3. Evaluation of the tools used in this study to modulate OGT expression.

Flies were raised at 25°C with control diet.

(A) qRT-PCR analyses of *gfat1* and *gfat2* mRNA levels in control (*act5c>RFP*) and *gfat2* knockdown (*act5c>gfat2-RNAi*) larvae. The knockdown efficiency of the *gfat1-RNAi* line was not evaluated as *act5c>gfat1-RNAi* animals could not survive to larval stage.

(B) qRT-PCR analyses of *hipk* and *ogt* mRNA levels in control (*act5c>GFP*), *ogt* knockdown (*act5c>ogt-RNAi*), and *ogt*-overexpressing (*act5c>ogt*) larvae.

(C) Western-Blot analyses of OGT protein levels in control (*act5c>GFP*), *ogt* knockdown (*act5c>ogt-RNAi*), *ogt* knockdown #2 (*act5c>ogt-RNAi #2*) and *ogt*-overexpressing (*act5c>ogt*) larvae. β-Tubulin was used as a loading control.

(D-E) Immunofluorescence staining of OGT (magenta in **D, E**; grey in **D'**, **E'**) using anti-OGT antibodies in larval wing imaginal discs. *en-Gal4* driver induces *UAS-ogt-RNAi* **(D)** or *UAS-ogt* **(E)** expression in the posterior compartments (marked by GFP). DAPI was used to stain DNA (blue). Scale bar, 50 µm.

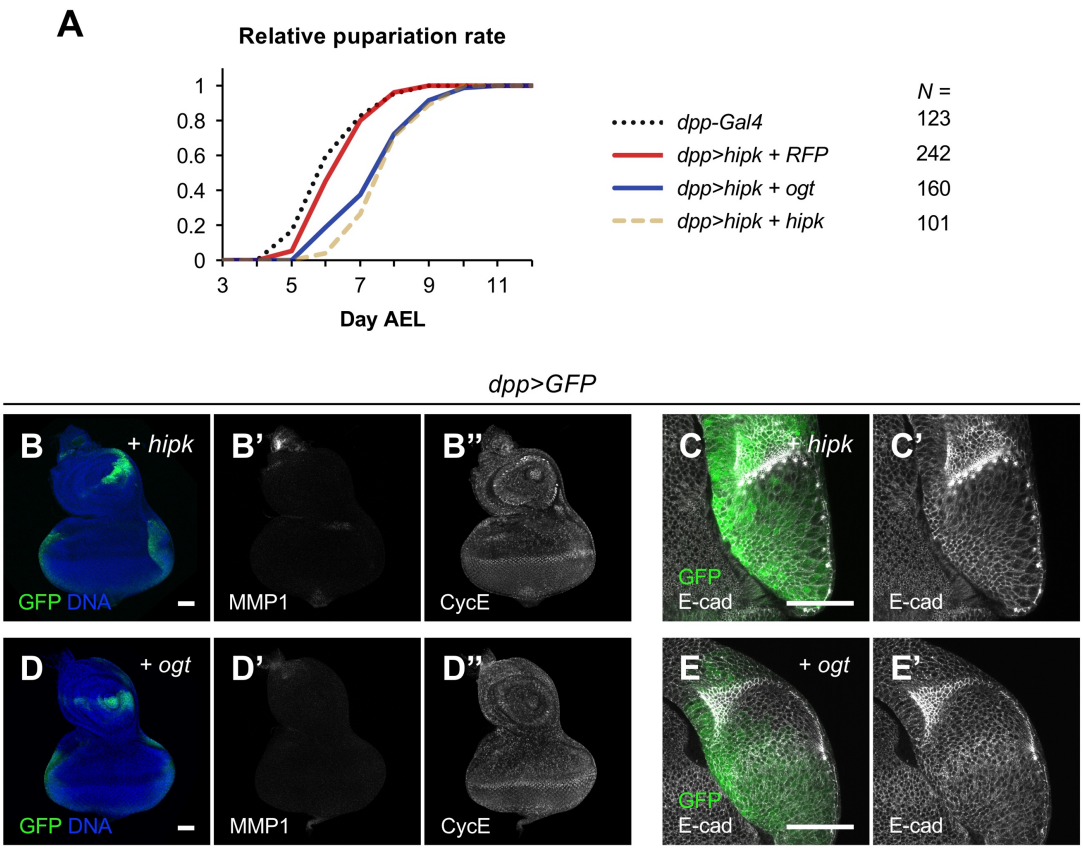

Fig. S4. OGT augments Hipk activity.

Flies were raised at 25°C with control diet.

(A) Relative pupariation rate of the flies of indicated genotypes revealing a developmental delay in larvae driven by a synergistic effect between Hipk and OGT, an effect mimicking that when two copies of Hipk are expressed. *N*, number of pupae counted. AEL, after egg laying.

(B-E) Staining of MMP1, CycE and E-cad in *hipk*-expressing eye-antennal discs (*dpp>GFP* + *hipk*) and *ogt*-expressing discs (*dpp>GFP* + *ogt*). No noticeable changes in MMP1, CycE or E-cad levels were observed when compared with control discs **(Fig. 2L, M, O)**. DAPI was used to stain DNA (blue). Scale bar, 50 μm.

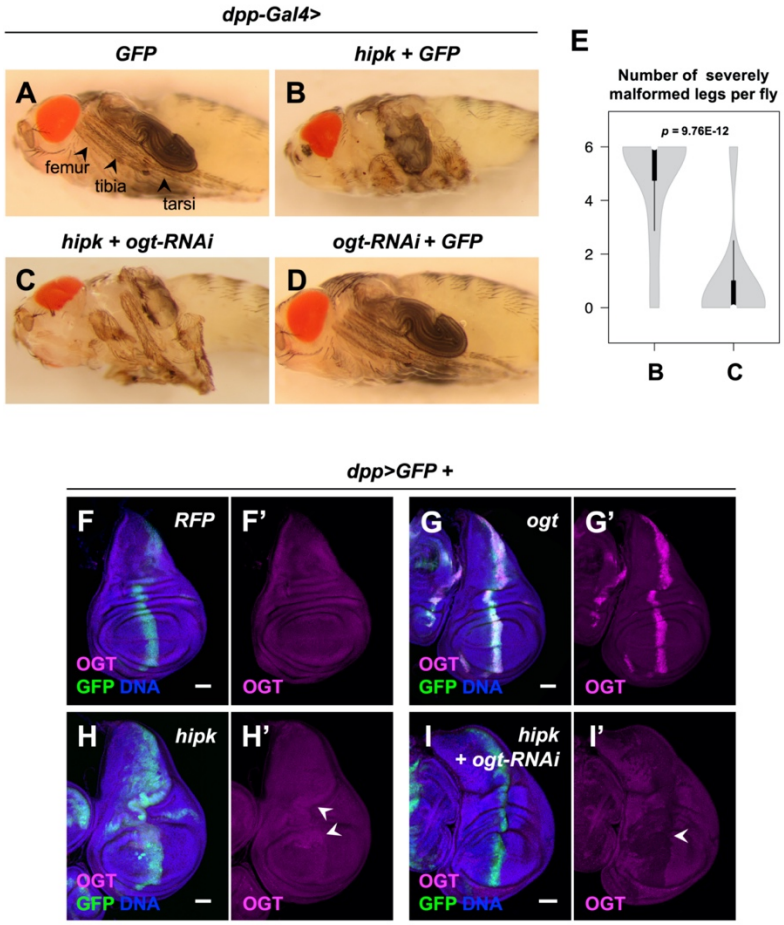

Fig. S5. OGT is required for Hipk activity.

Flies were raised at 29°C with control diet.

(A-D) Side views of the flies showing the leg phenotypes. **(A)** The adult legs of control flies were slender and mainly composed of three segments known as femur, tibia and tarsi. **(B)** The adult legs of *hipk*-overexpressing flies (*dpp>hipk + GFP*) were chubby with loss of segmentation. **(C)** Knockdown of *ogt* partially suppressed the severely malformed leg phenotype induced by elevated Hipk. **(D)** The adult legs of *ogt* knockdown flies (*dpp>ogt-RNAi + GFP*) appeared wild-type.

(E) Quantification of the severe leg malformation phenotype of the indicated animals. The letters **B-C** refer to the flies shown in **Fig. S5B-C**. Numbers of flies counted *N*: **B**: 36. **C**: 28. *p* value shown was calculated using unpaired two-tailed Student's *t*-test.

(F-I) Control (*dpp>GFP + RFP*) **(F)**, *ogt*-overexpressing (*dpp>GFP + ogt*) **(G)**, *hipk*-overexpressing (*dpp>GFP + hipk*) **(H)**, *hipk* and *ogt-RNAi* co-expressing (*dpp>GFP + hipk + ogt-RNAi*) **(I)** wing discs stained for OGT (magenta). GFP (green) marks the transgene-expressing cells. DAPI staining for DNA (blue) shows the tissue morphology. Scale bar, 50 μm. **(H)** White arrowheads mark the relatively small increases in OGT levels in *hipk*-overexpressing cells. **(I)** White arrowhead marks the loss of OGT staining in *hipk* and *ogt-RNAi* co-expressing cells.

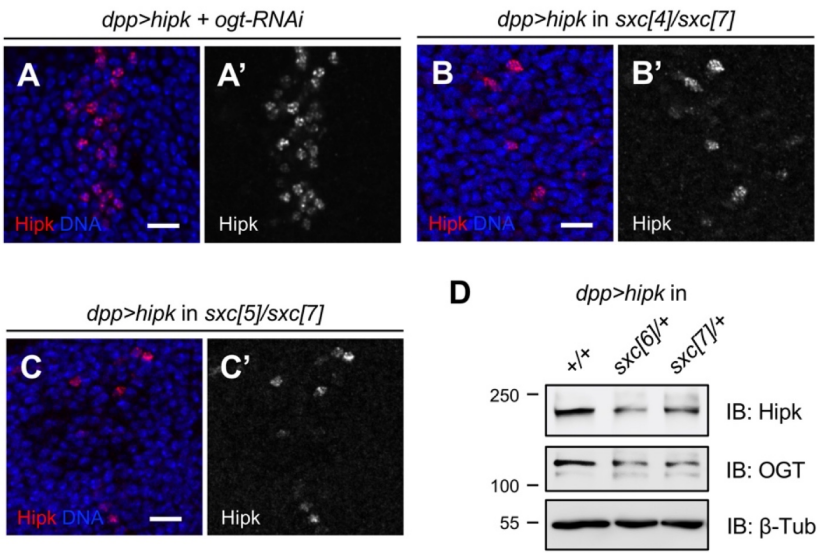

Fig. S6. Depletion of OGT reduces Hipk protein levels.

Flies were raised at 29°C with control diet.

(A-C) Compared with controls **(Fig. 4A)**, Hipk staining (red; grey in **A'**, **B'**, **C'**) in larval wing imaginal discs was reduced when *ogt* was knocked down **(A)**, in an *sxc[4]/sxc[7]* trans-heterozygous mutant background **(B)**, or in an *sxc[5]/sxc[7]* trans-heterozygous mutant background **(C)**. DAPI was used to stain DNA (blue). Scale bar, 10 μm.

(D) Western blot analyses showing that loss of one copy of the wild-type *ogt* (*sxc*) alleles led to reduced Hipk and OGT protein levels. β-Tubulin was used as a loading control.

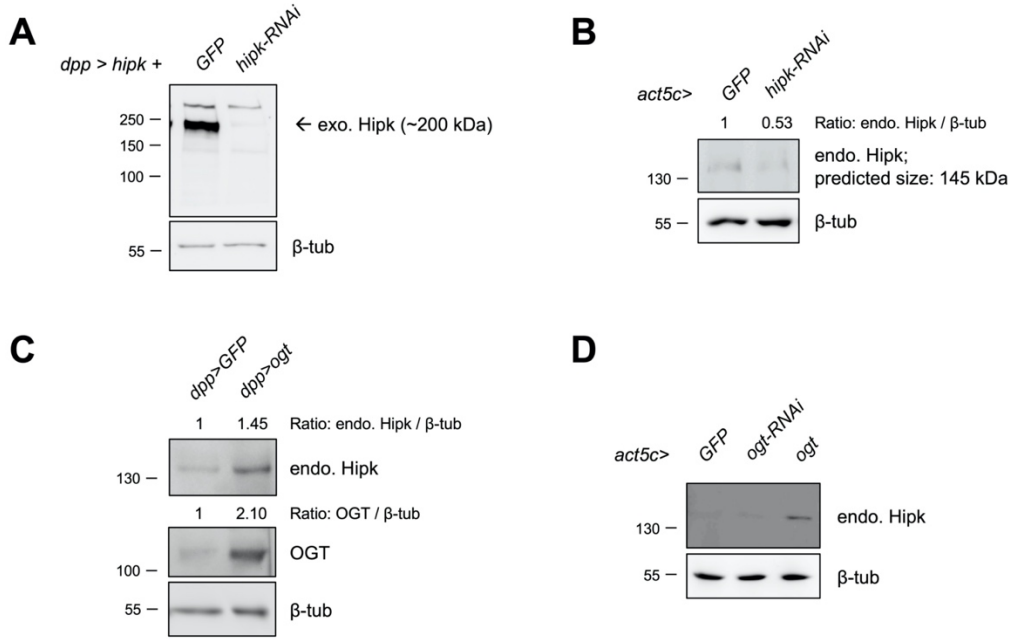

Fig. S7. OGT overexpression leads to accumulation of endogenous Hipk proteins.

(A) Validation of the anti-Hipk antibodies in the detection of exogenous Hipk proteins. Western-blot analyses using anti-Hipk antibodies to show exogenous Hipk proteins (at a molecular size of approximate 200 kDa) in protein lysates extracted from *dpp>hipk + GFP* and *dpp>hipk + hipk-RNAi* larval heads.

(B) Validation of the anti-Hipk antibodies in the detection of endogenous Hipk proteins. Western-blot analyses using anti-Hipk antibodies to show endogenous Hipk proteins (predicted molecular size: 145 kDa) in protein lysates extracted from control (*act5c>GFP*) and *hipk* knockdown (*act5c>hipk-RNAi*) larvae.

(C) Western-blot analyses using anti-Hipk antibodies to show endogenous Hipk proteins in protein lysates extracted from control (*dpp>GFP*) and *ogt*-overexpressing (*dpp>ogt*) larval heads.

(D) Western-blot analyses using anti-Hipk antibodies to show endogenous Hipk proteins in protein lysates extracted from control (*act5c>GFP*), *ogt* knockdown (*act5c>ogt-RNAi*) and *ogt* overexpressing (*act5c>ogt*) larvae.

β-Tubulin was used as a loading control.

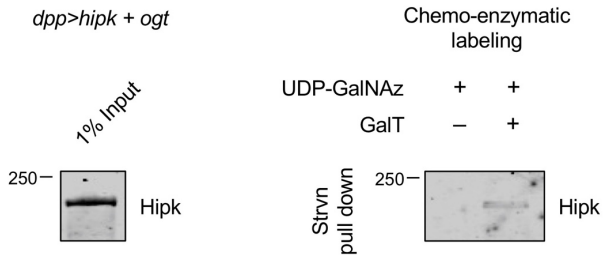

Fig. S8. GalT selectively labels Hipk with UDP-GalNAz.

Western blot analyses of Hipk following chemoenzymatic labeling with or without GalT, and Strvn precipitation using protein lysates from larvae co-expressing *hipk* and *ogt* (input).

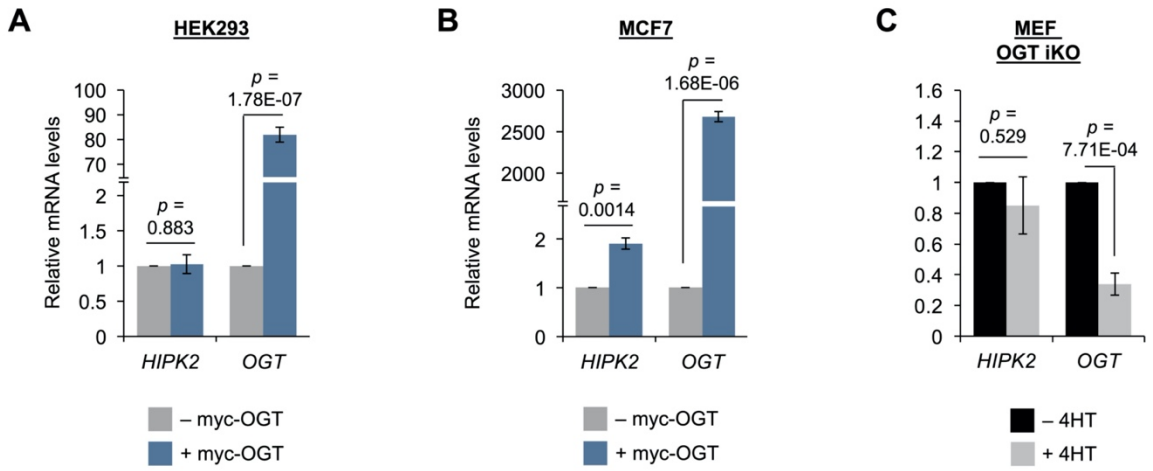

Fig. S9. Effects of OGT on the transcript levels of mammalian HIPK2.

(A) qRT-PCR analyses of *HIPK2* and *OGT* mRNA levels in HEK293 cells transfected with mock or myc-OGT. **(B)** qRT-PCR analyses of *HIPK2* and *OGT* mRNA levels in MCF7 cells transfected with mock or myc-OGT. **(C)** qRT-PCR analyses of *HIPK2* and *OGT* mRNA levels in an MEF OGT inducible knockout (iKO) cell line treated with mock or 4HT. *p* values were calculated using unpaired two-tailed Student's *t*-test.

A

	HIPK2-Replicate 1	HIPK2-Replicate 2
Total Protein ID	1017	947
Rank (by Sum PEP Score)	48	56
Protein Sequence Coverage	40%	41%
O-GlcNAc Sites	2 (T1009 and S1147)	3 (S852, S1008/T1009 and S1147)
Other O-GlcNAcylated Proteins	28	33

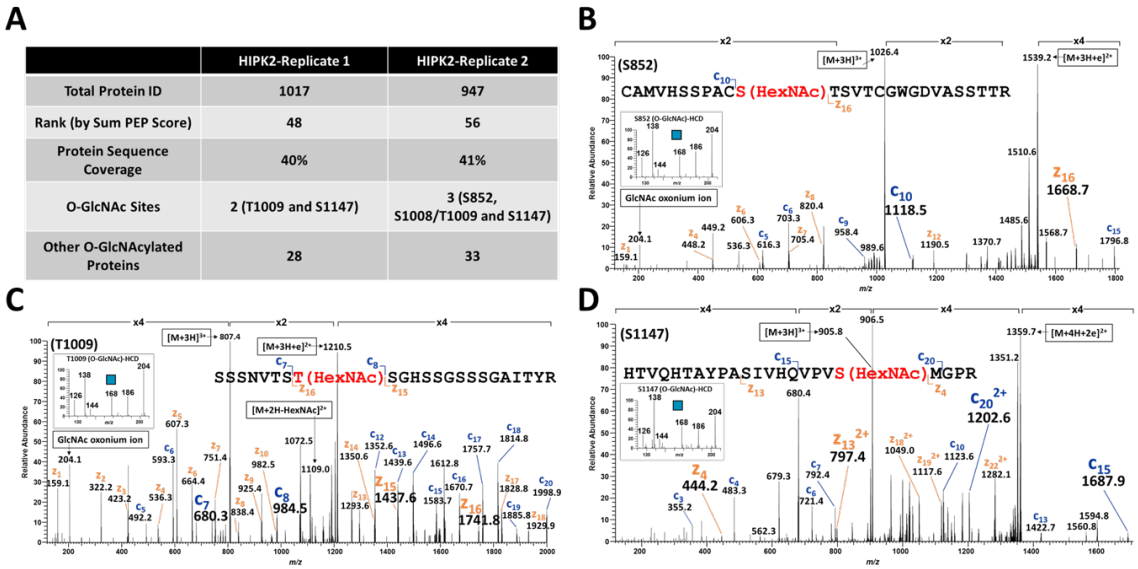

Fig. S10. Human HIPK2 is *O*-GlcNAc modified at multiple serine and threonine sites.

(A) Summary of the mass spectrometry results showing protein coverage and identification of O-GlcNAc sites (S852/T853, S1008/T1009 and S1147) obtained from two biological samples of purified HIPK2. **(B-D)** Representative EThcD MS/MS spectra for the three different O-GlcNAc modified HIPK2 peptides identified. The accompanying HCD MS/MS data each afforded the low mass characteristic ions that further identified the HexNAc as GlcNAc (insets).

Entry	Species	Peptide 1 (S852, T853)	Peptide 2 (S1008, T1009)	Peptide 3 (S1147)
Q9H2X6	Human	CAMVHSSPACSTSVTCGWGDVASSTTR	SSSNVTSTSGHSSGSSSGAITYR	HTVQHTAYPASIVHQVPVSMGPR
Q9QZR5	Mouse	CAMVHSSPACSTSVTCGWGDVASSTTR	SSSTVTSTSGHSSGSSSGAIAYR	HTVQHTAYPASIVHQVPVSMGPR
Q9WUM7	Golden hamster	CAMVHSSPACSTSVTCGWGDVASSTTR	SSSTVTSTSGHSSGSSSGAIAYR	HTVQHTAYPASIVHQVPVSMGPR
D3ZN85	Rat	CAMVHSSPACSTSLTCGWGDGASSTTR	SSSTVTSTSGHSSGSSSGAIAYR	HTVQHTAYPASIVHQVPVSMGPR
H2QVH2	Chimpanzee	CAMVHSSPACSTSVTCGWGDVASSTTR	SSSNVTSTSGHSSGSSSGAITYR	HTVQHTAYPASIVHQVPVSMGPR
F1PR67	Dog	CALVHSSPACSSSVTCGWGDGASSTTR	SSSNVTSTSGHSSGSSSGAIAYR	HTVQHTAYPASIVHQVPVSMGPR
F6XB80	Horse	CALVHSSPACSSSVTCGWGDGASSTAR	SSSNVTSTSGHSSGSSSGAVAYR	HTVQHTAYPASIVHQVPVSMGPR
H0V9Q0	Guinea pig	CAMAHSSPACSASVTCGWGDMASSTTR	SSSNVTSTSGHSSGSSSGAIAYR	HTVQHTAYPASIVHQVPVSMGPR
S6BAK9	Zebrafish	*No similar peptides found*	*No similar peptides found*	HAVQHASYPPGIVHQVPVSMGHR
Q9W0Q1	Fruit fly	*No similar peptides found*	*No similar peptides found*	PPLQVPPQQYVNVPVPVSMVEP

Fig. S11. The *O*-GlcNAc sites of HIPK2 are conserved in many mammalian species.

Searches and alignments of the *O*-GlcNAc sites (S852/T853, S1008/T1009 and S1147) of human HIPK2 with other species. The *O*-GlcNAc sites are labeled in red. In simpler organisms like zebrafish and fruit fly, only S1147 seems conserved. Conserved residues are labeled in grey, and non-conserved residues in brown.

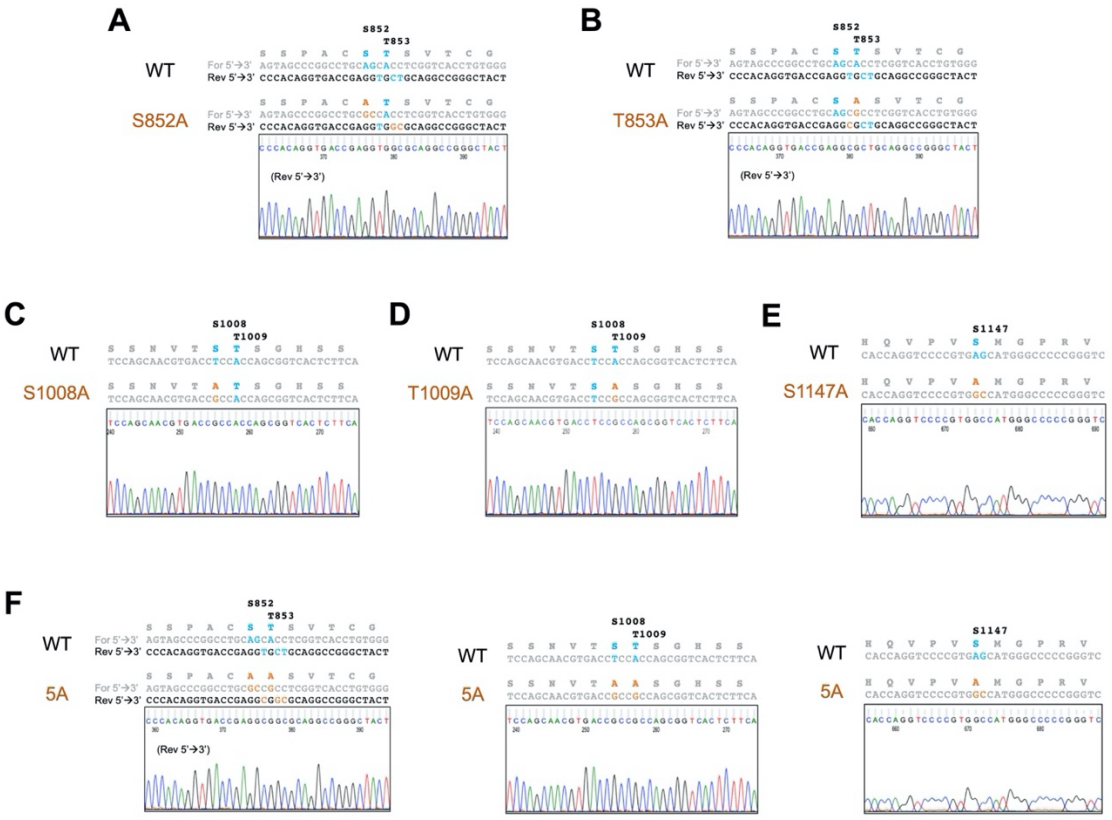

Fig. S12. Replacements of HIPK2 *O*-GlcNAc sites by alanine are confirmed by sequencing.

Sequencing data confirm the replacements of *O*-GlcNAc modified serine and threonine sites by alanine residues in individual single alanine mutants **(A-E)** and a quintuplet alanine (5A) mutant **(F)**. Wild-type *O*-GlcNAc modified residues and the corresponding nucleotides are shown in light blue, and replaced residues/mutated nucleotides in brown.

Table S1. Primers used for qRT-PCR.

Species	Gene	Forward sequence (5'→3')	Reverse sequence (5'→3')
Drosophila	rp49	ATCGGTTACGGATCGAACAA	GACAATCTCCTTGCGCTTCT
Drosophila	hipk	GCACCACAACTGCAACTACG	ACGTGATGATGGTGCGAACTC
Drosophila	ogt	GCTATACGCCTGGGAACAAA	CCTTTGGCATACTGTGAGCA
Human	HPRT1	GCTATAAATTCTTTGCTGACCTGCTG	AATTACTTTTATGTCCCCTGTTGACTGG
Human	HIPK2	AATAGAGCCGAGTTCCAACTGG	GTCTGCTCGTAAGGTAGGCTT
Human	OGT	CCTGGGTCGCTTGGAAGA	TGGTTGCGTCTCAATTGCTTT
Human	α-Tubulin	CCAAGCTGGAGTTCTCTA	CAATCAGAGTGCTCCAGG
Mouse	β-Tubulin	CTCCACCCAGAGAATGCACG	GCGGAGCTGATCGAAAATGTC
Mouse	HIPK2	TGCTTGACTTCCCCCATAGTG	CTTGCAAATCTCCATGTTTTGG

Table S2. Primers used for site-directed mutagenesis

Mutation site(s)	**Forward sequence (5'→3')**	**Reverse sequence (5'→3')**
S852A	CAGTAGCCCGGCCTGCGCCACCTC GGTCACCTG	CAGGTGACCGAGGTGGCGCAGGCC GGGCTACTG
T853A	CCCGGCCTGCAGCGCCTCGGTCAC CTG	CAGGTGACCGAGGCGCTGCAGGCC GGG
S852A, T853A	CAGTAGCCCGGCCTGCGCCGCCTC GGTCACCTGTGG	CCACAGGTGACCGAGGCGGCGCAG GCCGGGCTACTG
T1009A	CAGCAACGTGACCTCCGCCAGCGG TCACTCTTC	GAAGAGTGACCGCTGGCGGAGGTC ACGTTGCTG
S1008A, T1009A	CAGCAACGTGACCGCCGCCAGCGG TCACTCTTC	GAAGAGTGACCGCTGGCGGCGGTC ACGTTGCTG
S1147A	CCACCAGGTCCCCGTGGCCATGGG CCCCCGGGTC	GACCCGGGGGCCCATGGCCACGGG GACCTGGTGG

SI References

1. Musselman LP, et al. (2011) A high-sugar diet produces obesity and insulin resistance in wild-type Drosophila. *Dis Model Mech* 4(6):842–9.
2. Blaquiere JA, Wong KKL, Kinsey SD, Wu J, Verheyen EM (2018) Homeodomain-interacting protein kinase promotes tumorigenesis and metastatic cell behavior. *Dis Model Mech* 11(1). doi:10.1242/dmm.031146.
3. Lee W, Swarup S, Chen J, Ishitani T, Verheyen EM (2009) Homeodomain-interacting protein kinases (Hipks) promote Wnt/Wg signaling through stabilization of beta-catenin/Arm and stimulation of target gene expression. *Development* 136(2):241–51.
4. Sinclair DAR, et al. (2009) Drosophila O-GlcNAc transferase (OGT) is encoded by the Polycomb group (PcG) gene, super sex combs (sxc). *Proc Natl Acad Sci U S A* 106(32):13427–32.
5. Gambetta MC, Oktaba K, Müller J (2009) Essential Role of the Glycosyltransferase Sxc/Ogt in Polycomb Repression. *Science (80-)* 325(5936):93–96.
6. Liu T-W, et al. (2017) Genome-wide chemical mapping of O-GlcNAcylated proteins in Drosophila melanogaster. *Nat Chem Biol* 13(2):161–167.
7. Rappsilber J, Mann M, Ishihama Y (2007) Protocol for micro-purification, enrichment, pre-fractionation and storage of peptides for proteomics using StageTips. *Nat Protoc* 2(8):1896–1906.